Chromatin landscape dynamics of the *Il4–Il13* locus during T helper 1 and 2 development

Aurélie Baguet and Mark Bix*

Department of Immunology, University of Washington, Seattle, WA 98195-7650

Edited by Stanley M. Gartler, University of Washington, Seattle, WA, and approved June 17, 2004 (received for review May 11, 2004)

Il4 **and** ***Il13*** **encode the canonical T helper 2 (T_H2) cytokines responsible both for promoting immune responses against extracellular pathogens and, when misregulated, causing allergic and autoimmune disease. The expression potential of these genes undergoes developmentally programmed repression and enhancement during commitment of naïve $CD4^+$ T cells to the mature T helper 1 (T_H1) and T_H2 fates, respectively. Thus, like the globin locus, the T_H2 cytokine locus provides a highly tractable system to study a developmental fate choice leading to alternative transcriptional states of either silence or permissivity. We used quantitative chromatin immunoprecipitation and RT-PCR to correlate changes in the transcriptional states of** ***Il4*** **and** ***Il13*** **with markers of permissive chromatin across the** ***Il4–Il13*** **locus in naïve $CD4^+$ T cells undergoing T_H1 and T_H2 differentiation. We provide evidence that DNaseI hypersensitive site V in the** ***Il4*** **3′ enhancer is the likely target for signals maintaining** ***Il4*** **and** ***Il13*** **transcriptional permissivity in naïve cells. We also demonstrate rapid acquisition of differences in H3 acetylation between T_H1- and T_H2-primed cells, indicating a developmentally early role for cytokine signaling in the process of T_H cell fate determination. Finally, we show that transcriptional repression correlates with the disappearance of permissive H3 modifications from everywhere in the** ***Il4–Il13*** **locus except hypersensitive site IV, suggesting a critical role for this element in the maintenance of transcriptional repression. Our findings are consistent with a progressive regulatory element activation/deactivation model of T_H1/T_H2 development.**

Depending on the nature of signals encountered during initial activation, naïve $CD4^+$ T cells can be instructed to differentiate toward a variety of effector and memory cell fates, distinguished primarily by the potential to express different patterns of cytokine genes. Those that have received the most attention are called T helper 1 (T_H1) and T_H2. The physically clustered T_H2 cytokine genes *Il4*, *Il13*, and *Il5* are transcriptionally repressed in T_H1 cells and permissive in T_H2 cells; the converse is true for the unlinked T_H1 cytokine gene *Ifng*. Because different microbes and tissue environments require different effector strategies, proper regulation of this developmental fate choice during immune responses *in vivo* is critical for the effective control of infectious pathogens, as well as for preventing harmful autoimmune and allergic diseases (1, 2).

Elucidation of the molecular pathways regulating the developmentally programmed changes in *Il4* and *Il13* transcriptional state that occur with T_H development will benefit from a detailed understanding of the *cis*-acting genetic elements that coordinate their transcriptional behavior. There are 13 hypersensitive site (HS) clusters that have been mapped within the *Il4–Il13* locus (3, 4). These can be classified into three groups based on their lineage specificity and requirement for cellular activation: (*i*) T_H2-specific/constitutive, (*ii*) T_H2-specific/activation-dependent, and (*iii*) naïve/T_H1/T_H2-shared/constitutive. It is likely that these HSs (and perhaps others more distal; ref. 5) comprise the complete set of regulatory elements responsible for integrating upstream signals into coordinated responses that developmentally alter the transcriptional potential of *Il4* and *Il13*. These responses are likely to involve the recruitment and deployment of both chromatin modifying and RNA polymerase II recruitment/transcription-promoting activities. Targeted deletions have recently demonstrated that several of the HSs (V/Va and S1/S2) are indeed important for *Il4* and *Il13* expression in T_H2 cells (6, 7). However, it is still not known, for each successive development stage, which elements are active, the upstream signaling pathways to which each responds, and the downstream activities each coordinates.

The flexible amino termini of nucleosomal histones harbor multiple residues that can undergo a variety of posttranslational modifications, including acetylation, methylation, and phosphorylation. Combined with the octameric structure of the nucleosomal core, this flexible modification system harbors tremendous combinatorial diversity and information coding potential (the so-called histone code) that can endow discrete genetic intervals with specific functional properties (8). For histone H3, posttranslational modifications can be classified into those associated with chromatin that is transcriptionally repressed (lysine 9 or 27 di- and trimethylation) or transcriptionally permissive [lysine 9/14 acetylation (AcK9/14), lysine 4 dimethylation (2MeK4) and serine 10 phosphorylation (PhS10)] (reviewed in ref. 9). Along a given genetic interval, histone-modifying factors recruited to specific regulatory elements create a dynamic pattern of histone modification specificities and intensities. These, in turn, influence the transcriptional behavior of associated genes by creating or destroying binding platforms for transcriptional activators, repressors, nucleosome remodeling, and chromatin packaging machinery (10). Thus, by characterizing the dynamic chromatin landscape of the *Il4–Il13* locus during T_H1 and T_H2 development and correlating this to the evolving transcriptional states of *Il4* and *Il13* one may be able to infer for each given element: (*i*) the developmental stages at which it is active; (*ii*) the nature of histone-modifying enzymes it may recruit; and (*iii*) the transcription-modifying activities it may regulate.

Recent evidence indicates that the ability of naïve $CD4^+$ T cells to express *Il4* is epigenetically programmed during thymic development coincident with CD4/CD8 lineage commitment (11). During subsequent peripheral maturation steps, this potential is reported to undergo partial repression through mechanisms that involve *Il4–Il13* locus DNA methylation (11). Despite the accumulation of repressive DNA methylation marks, the *Il4–Il13* locus in naïve $CD4^+$ T cells remains transcriptionally permissive. However, permissive H3 modifications at the *Il4–Il13* locus of naïve $CD4^+$ T cells have not been detected (12, 13), begging the question: how is permissivity maintained? Our analysis of the dynamic pattern of permissive H3 modifications at the *Il4–Il13* locus during T_H1 and T_H2 development implicates the T_H2-specific/constitutive HS_V 3′ of the *Il4* gene as the likely recipient of permissivity-inducing signals. In addition, we show that locus-wide changes in permissive modifications that have occurred 48 h after the onset of activation differ greatly in magnitude and stability depending on priming conditions. T_H2-priming is associated with high-level/stable and T_H1-priming with low-level/transient increases in permissive H3

This paper was submitted directly (Track II) to the PNAS office.

Abbreviations: ChIP, chromatin immunoprecipitation; T_H, T helper; HS, hypersensitive site; PMA, phorbol 12-myristate 13-acetate.

*To whom correspondence should be addressed. E-mail: mbix@u.washington.edu.

www.pnas.org/cgi/doi/10.1073/pnas.0403334101

modifications, indicating that cytokine signaling influences chromatin structure earlier than had previously been suggested (12, 13). We also discovered a significant delay in the occurrence of T_H1-priming-dependent *Il4* and *Il13* transcriptional repression that correlated with the disappearance of permissive H3 modifications from everywhere in the *Il4–Il13* locus except HS_{IV}, suggesting a role for this element in the maintenance of transcriptional repression. We discuss our findings in the context of a progressive regulatory element activation/deactivation model of T_H1/T_H2 development.

Materials and Methods

Cell Lines. D10.G4 (14) and A.E7 (15) were grown in RP10 (RPMI medium 1640 supplemented with 2 mM L-glutamine/25 mM Hepes/0.05 mM 2-mercaptoethanol/50 units/ml penicillin/50 μg/ml streptomycin/10% FBS). Both clones were maintained by periodic stimulation with irradiated AKR/J splenocytes and antigen (D10.G4, conalbumin; and A.E7, pigeon cytochrome *c*). Resting clones were harvested at least 5 days after the last stimulation. Resting cells were activated by 4-h culture with phorbol 12-myristate 13-acetate (PMA) (5 ng/ml) and ionomycin (250 ng/ml). NIH3T3 cells were grown in DMEM10 (DMEM supplemented with 4 mM L-glutamine/4.5 g/liter glucose/1.5 g/liter sodium bicarbonate/50 units/ml penicillin/50 μg/ml streptomycin/10% FBS).

Naïve T Cell Purification. $CD4^+CD62L^{Hi}$ naïve T cells were generated by two sequential AutoMACS purification steps. First, $CD4^+$ T cells were isolated from combined lymph node and spleen cell suspensions stained with FITC-anti-CD4 antibody (GK1.5, BD/Pharmingen) followed by anti-FITC MultiSort MicroBeads (Miltenyi Biotec, 130-058-701). After cleavage of the MultiSort MicroBeads, $CD4^+CD62L^{Hi}$ cells were purified from $CD4^+$ T cells stained with anti-CD62L MicroBeads (Miltenyi Biotec, 130-049-701). In Fig. 2*D*, initial purification of $CD4^+$ T cells was performed by negative selection using the $CD4^+$ T cell Isolation kit (Miltenyi Biotec, 130-090-860). Purity of $CD4^+CD62L^{Hi}$ T cells as determined by fluorescence-activated cell sorter (FACS) analysis was $\geq$98% (positive selection for $CD4^+$) and $\geq$95% (negative selection for $CD4^+$).

T_H1 and T_H2 Cultures. Primary T_H cultures were generated by using 4- to 6-week-old BALB/c mice (The Jackson Laboratories) housed under specific pathogen-free conditions at the University of Washington, Seattle. $CD4^+$ T cells, AutoMACS purified from combined lymph node and spleen cell suspensions stained with anti-CD4 MicroBeads (Miltenyi Biotec, 130-049-201), were $\geq$98% CD4 positive as determined by fluorescence-activated cell sorter analysis. Splenic antigen-presenting cells (APCs) were prepared by complement-mediated lysis using anti-Thy1 (J1j, American Type Culture Collection) and a combination of rabbit and guinea pig complement and given 3,000 rads before use. T_H cell cultures were seeded at a ratio of 1:5 (T cell/APC) with anti-CD28 (25 μg/ml, 37N) and anti-T cell receptor β (2.5 μg/ml, H57–597). In addition, T_H1 cultures contained recombinant mouse IL12 (1 ng/ml, R & D Systems) and anti-IL4 (10 μg/ml, 11B11) whereas T_H2 cultures contained recombinant mouse IL4 (30 ng/ml, Leinco Technologies), anti-IL12 (4.5 μg/ml, C17.8), and anti-IFNγ (10 μg/ml, R46A2). Cultures, harvested at 48 h, were stimulated as described above for the cloned cell lines.

RT-PCR. RNA was isolated with STAT60, and contaminating genomic DNA was removed by using RNase-Free DNase (Ambion, 1906). Random hexamer-primed cDNA was generated by using the Superscript II RNase H^- Reverse Transcriptase kit (Invitrogen, 18064-014). Real-time PCRs were performed and analyzed on a Stratagene MX4000. The PCR buffer contained 10 mM Tris (pH 8.3), 50 mM KCl, 4.5 mM $MgCl_2$, 0.01% Tween 20, 0.3% DMSO, 0.0025% SYBR Green I solution (Molecular Probes, S-7563), 50 nM each primer (Table 1, which is published as supporting information on the PNAS web site), and *Taq* polymerase (Promega)/anti-*Taq* antibody (Clontech) conjugate per 25 μl of reaction. Cycling conditions were: 94°C for 4 min followed by 40 cycles of 94°C for 20 sec, 61°C for 1 min and 72°C for 40 sec. PCR efficiencies were optimized in pilot experiments. C_T values for no reverse transcriptase (NRT) controls were at least 4-fold higher than experimental samples, corresponding to <6% background. More often, NRT background was <0.8%. The only exception was site N with 17% background. For a given cDNA, relative abundance of each target was normalized to *Hprt* according to the formula: $2^{-\Delta CT}$, where $\Delta C_T = C_T^{TARGET} - C_T^{HPRT}$. *Hprt*-normalized target signals were expressed relative to expression in NIH3T3 fibroblasts according to the formula: $2^{-\Delta\Delta CT}$, where $\Delta\Delta C_T = \Delta C_T^{SAMPLE} - \Delta C_T^{NIH3T3}$. Thus 1 arbitrary unit (AU) corresponds to the relative level of a given target in NIH3T3 fibroblasts.

Chromatin Immunoprecipitation (ChIP) Assays. Approximately 3×10^7 cells were used per ChIP (for additional details, see *Supporting Text*, which is published as supporting information on the PNAS web site). DNA recovered from an aliquot of sheared chromatin was used as the "input" sample. The remaining chromatin was precleared with protein A- and protein G-agarose (Upstate Biotechnologies, catalogue nos. 16-156 and 16-266) and then incubated with one of three antibodies overnight at 4°C [anti-AcK9/14-H3, catalog no. 06-599; anti-M3K4-H3, catalog no. 07-030; anti-PhS10-H3, catalog no. 05-598; Upstate Biotechnology; all used at 2 μg/ml). Input DNA and DNA recovered after IP were quantified by using picogreen fluorescence (Molecular Probes). Equivalent mass of IP and input DNA was analyzed by real-time PCR as described above for RT-PCR with the following modifications. *Taq* polymerase was from Qiagen (Hot Start) and cycling conditions were 94°C for 15 min followed by 40 cycles of 94°C for 20 sec, 61°C for 1 min, and 72°C for 40 sec. Data are presented as the ratio of $2^{-C_T^{IP}}$ to $2^{-C_T^{input}}$.

Results

Transcriptional Response of Naïve, T_H1, and T_H2 Cells. We used quantitative RT-PCR to characterize the 4-h PMA/ionomycin-induced transcriptional response of *Kif3a*, *Il4*, *Il13*, and *Rad50* in $CD4^+CD62L^{Hi}$ naïve T cells, 48-h T_H1- and T_H2-primed $CD4^+$ T cells, the T_H1 clone A.E7, and the T_H2 clone D10.G4. A.E7 and D10.G4 are well established models of the fully polarized T_H1 and T_H2 fates, respectively (14, 15). As expected, naïve cells induced both cytokine genes, although to levels reduced >200-fold compared to the T_H2 clone D10.G4 (Fig. 1*B*). Surprisingly, inducible *Il4* and *Il13* expression in 48-h T_H1-primed cells remained at (*Il4*) or increased slightly above (*Il13*) the level detected from activated naïve cells (Fig. 1*A*). Transcriptional repression of *Il4* and *Il13* was detected only in the T_H1 clone A.E7, representing a terminal stage of T_H differentiation (Fig. 1*A*). In contrast to the developmentally delayed onset of transcriptional repression, enhancement of inducible *Il4* and *Il13* expression occurred rapidly with T_H2-priming, approaching (*Il4*) or surpassing (*Il13*) levels detected in the T_H2 clone D10.G4 by 48 h of priming (Fig. 1*B*). Expression of *Kif3a* and *Rad50* were similar at all stages of development regardless of priming conditions (Fig. 1), indicating that the flanking genes are somehow insulated from the regulatory events governing the *Il4–Il13* locus.

H3 Modifications in $CD4^+CD62L^{Hi}$ Naïve T Cells. To determine whether the developmentally programmed changes in *Il4* and *Il13* transcriptional state are linked to chromatin-level changes, we used ChIP to assess posttranslational modification of histone H3 across the *Il4–Il13* locus. We focused our analysis on the permissive chromatin modifications AcK9/14 and 2MeK4. Real-time PCR was used to quantitate the relative enrichment of specific target sequences in

IMMUNOLOGY

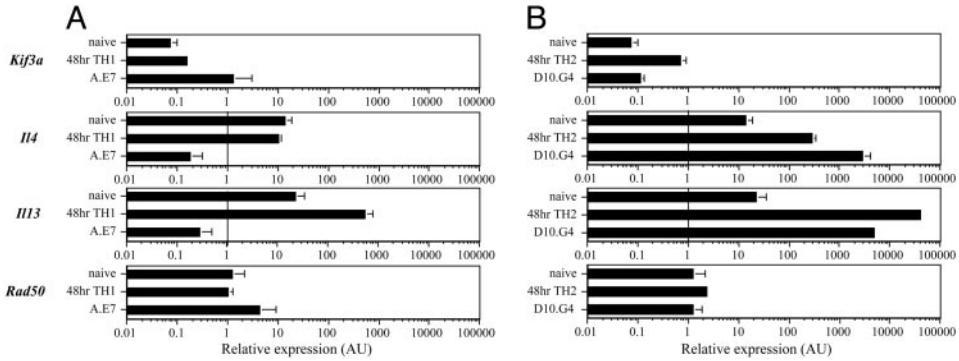

Fig. 1. *Kif3a*, *Il4*, *Il13*, and *Rad50* mRNA expression in developing T_H1 and T_H2 cells. $CD4^+CD62L^{Hi}$ naïve T cells (*A* and *B*), CD4 T cells primed for 48 h in T_H1 (*A*) or T_H2 (*B*) skewing condition, the T_H1 clone A.E7 (*A*), and the T_H2 clone D10.G4 (*B*) were harvested for RNA after 4 h of activation with PMA and ionomycin. Relative expression of *Kif3a*, *Il4*, *Il13*, and *Rad50* was determined by quantitative real-time PCR. The ratio of *Hprt*-normalized expression in T cells and NIH3T3 cells is depicted in arbitrary units (AU). Error bars are SEM of $n \geq 2$.

equivalent amounts of DNA obtained from unprecipitated and precipitated chromatin (Fig. 6, which is published as supporting information on the PNAS web site). We designed PCR primer pairs (probes A–P in Table 1) targeting 17 sites, aiming to cover the locus uniformly and to sample regions known to be functionally, structurally, or computationally implicated in cytokine regulation (Fig. 2; probes A–P). These regions include the *Il4* 3′ enhancer comprising the T_H2-specific/constitutive HS_V and T_H2-specific/activation-dependent HS_{Va} (4, 7, 16), the CNS1 enhancer (a phylogenetically conserved region encompassing the clustered T_H2-specific/constitutive HS_{S1} and HS_{S2}; ref. 17), and the *Il4* intronic enhancer encompassing the T_H2-specific/constitutive HS_{III} and HS_{II} (4, 18). We also examined the T_H2-specific/constitutive *Il4* promoter-proximal HS_I and promoter-distal HS_0 (4) and *Il13* promoter-proximal HS_2 and promoter distal HS_1 (3). Finally, we monitored HS_{IV} and HS_{S3}, naïve/T_H1/T_H2–shared/constitutive HSs immediately downstream of *Il4* and *Il13*, respectively (3, 4, 17). Some regions were also chosen simply to provide extended coverage of the locus.

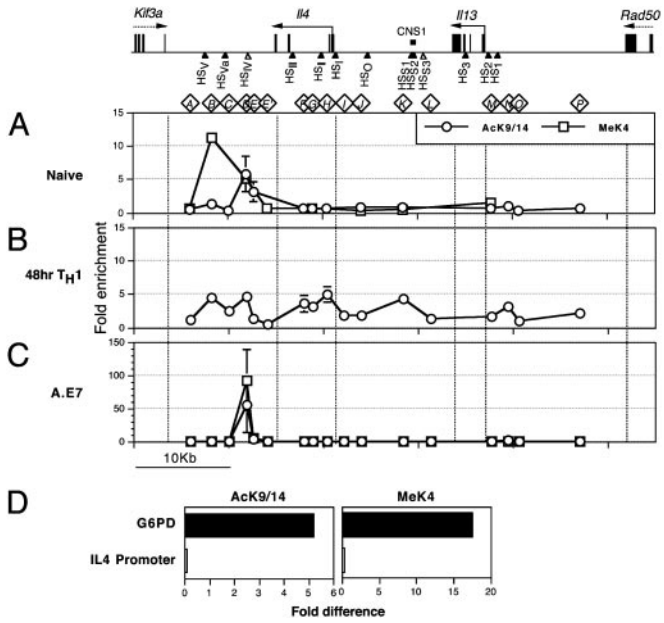

Fig. 2. Permissive histone H3 modification at the *Il4–Il13* locus during T_H1 development. Shown are ChIP plots depicting fold-enrichment for AcK9/14 (circles) and 2MeK4 (squares) across the *Il4–Il13* locus in $CD4^+CD62L^{Hi}$ naïve T cells (*A*), 48-h T_H1-primed $CD4^+$ T cells (*B*), and resting A.E7 cells (*C*). Error bars are SEM of $n \geq 2$ except for the following where $n = 1$: naïve (AcK9/14, sites F, G, H and P; 2MeK4, sites A, E′, and J) and A.E7 (AcK9/14, sites B, C E′, F, I, and L; 2MeK4, sites E′, I, and L). 2MeK4 data are not shown for 48-h-primed cells. At the top of the figure is a physical map of the chromosome 11 *Kif3a–Il4–Il13–Rad50* locus. Horizontal black arrows represent complete (solid lines) or partial (dotted lines) transcription units. Tall black rectangles represent exons. Arrowheads indicate the location of T_H2-specific/constitutive (filled symbols) and T_H2-specific/activation-dependent (open symbols) DNase I HSs. The small black rectangle represents a region of high sequence conservation between mouse and human (CNS1). Diamond-encased letters (A–P) represent the names and locations of PCR primer pairs. Dotted vertical lines in each plot bracket the locations of transcription units.

We began by isolating $CD4^+CD62L^{Hi}$ naïve T cells from spleen and lymph nodes of young BALB/c mice and processing them for ChIP with an antibody to AcK9/14. No AcK9/14 was detected at HS_V and CNS1 (Fig. 2*A*; probes B and K), corroborating earlier studies (12, 13). Additional sites not previously examined in naïve cells (HS_{Va}, HS_{III}, HS_{II}, HS_0, HS_2, HS_1, the *Kif3a*-proximal region, and the *Rad50*-proximal region) also lacked AcK9/14 (Fig. 2*A*; probes A–C, F–H, J, and M–P). HS_{IV} 3′ of *Il4* was the only region where AcK9/14 was detected (Fig. 2*A*; probe D). HS_{IV} has been reported to lack AcK9/14 in naïve cells (12). Differences in the precise regions targeted for PCR analysis or in the sensitivity of the quantitative assay used here and the qualitative assay used in earlier studies may account for the discrepancy. Thus, HS_{IV} appears to be the sole focus of preexisting AcK9/14 at the *Il4–Il13* locus in naïve T cells. However, because the T_H1 clone A.E7 also contains permissive H3 modifications at this site (Figs. 2*C* and 5, probe D), by itself, H3 modification at HS_{IV} is insufficient to explain the transcriptional permissivity of *Il4* and *Il13* in naïve T cells.

A recent study reported the occurrence of AcK9/14 at the *Il4* promoter in naïve $CD4^+$ T cells and suggested that mechanistically this modification might be responsible for *Il4* transcriptional permissivity (19). Although, as shown in Fig. 2*A*, our *Il4* promoter-proximal probe J that failed to detect histone acetylation was only 2.5 kb distal to the location of the PCR primer pair used in that study, we could not exclude the possibility that we had missed a nearby peak of acetylation. To address this, we purified $CD4^+CD62L^{Hi}$ naïve T cells and analyzed these by ChIP using an AcK9/14-specific antibody and PCR primers identical to those described by Grogan *et al.* (19). Despite strong AcK9/14 enrichment at the control *G6pd* locus, we were unable to detect any signal at the *Il4* promoter (Fig. 2*D*). Similarly, ChIP analysis of naïve cells with a 2MeK4-specific antibody also failed to reveal enrichment at this site despite a strong *G6pd* signal (Fig. 2*D*). We conclude that permissive chromatin modifications do not occur at the *Il4* promoter in naïve T cells.

To search for other changes that might still explain the transcriptional permissivity of *Il4* and *Il13* in naïve T cells, we extended our

2MeK4 ChIP-scan to the remainder of the *Il4–Il13* locus. The distribution of 2MeK4 we observed was nearly identical to that of AcK9/14, being mainly restricted to HS_{IV} (Fig. 2*A*; probe D). Like AcK9/14, 2MeK4 at HS_{IV} was also detected in T_H1 cells (Fig. 2*C*; probe D), further indicating that, by itself, this site does not play a role in maintaining *Il4* and *Il13* transcriptional permissivity. By contrast, at HS_V in the *Il4* 3′ enhancer, where no AcK9/14 had been detected, we found 2MeK4 to be enriched in naïve T cells (Fig. 2*A*; probe B). Permissive modifications at HS_V also occurred in a T_H2 but not in a T_H1 clone (Figs. 2*C* and 3*C*; probe B). Furthermore, 48-h T_H1-primed cells showed a significant decrease relative to naïve cells in 2MeK4 at HS_V (data not shown). Thus, the developmental dynamics of 2MeK4 suggests that HS_V may play a role in mediating the transcriptional permissivity of *Il4* and *Il13* in naïve $CD4^+$ T cells.

H3 Modifications in Developing T_H1 Cells. We hypothesized that the developmentally delayed onset of *Il4* and *Il13* transcriptional repression that occurs with T_H1-priming (Fig. 1*A*) would be linked to underlying features in the chromatin landscape of the *Il4–Il13* locus. To test this hypothesis, purified $CD4^+$ T cells from young BALB/c mice cultured for 48 h in T_H1-priming conditions were ChIP-scanned for AcK9/14. Compared to naïve T cells, we detected small increases in AcK9/14 (all <5-fold) at the *Il4* 3′, intronic and CNS1 enhancers and the *Il4* and *Il13* promoter-proximal regions (Fig. 2 *A* and *B*; probes B, C, F–K, M, N, and P). By contrast, no change was detected at HS_{IV} (Fig. 2 *A* and *B*; probe D). Thus, relative to naïve T cells, slightly increased *Il4* and *Il13* transcriptional permissivity in 48-h T_H1-primed cells correlate with modest increases in AcK9/14 levels across most of the *Il4–Il13* locus.

To assess the chromatin structural correlates of *Il4* and *Il13* transcriptional repression, we analyzed the T_H1 clone A.E7. Resting cells were ChIP-scanned with antibodies that detect AcK9/14, 2MeK4, and PhS10. All three markers of permissive chromatin were almost completely absent from the *Il4–Il13* locus (Figs. 2*C* and 5). The sole exception was HS_{IV}, where striking enrichment for all three permissive markers was focused in a sharp peak (Figs. 2*C* and 5; probe D). Permissive H3 modifications at HS_{IV}, like DNase I hypersensitivity (4), were lineage restricted as indicated by their absence from fibroblast lineage NIH3T3 cells (see Fig. 5 and data not shown for AcK9/14 and 2MeK4). Thus, the repressed transcriptional state of *Il4* and *Il13* correlates with the disappearance of permissive H3 modifications from everywhere in the *Il4–Il13* locus, except at HS_{IV}, where levels increased.

H3 Modifications in Developing T_H2 Cells. The inverse correlation between transcriptional repression and permissive H3 modifications seen across most of the *Il4–Il13* locus with T_H1 development suggested that the enhanced *Il4* and *Il13* transcriptional response seen with T_H2-priming would be positively correlated with permissive H3 modifications. To test this, purified $CD4^+$ T cells from young BALB/c mice cultured in T_H2-priming conditions for 48-hours were ChIP-scanned for AcK9/14. Relative to naïve T cells, we detected increased AcK9/14 levels at the *Il4* 3′, intronic and CNS1 enhancers and the upstream regions of both *Il4* and *Il13* (Fig. 3*B*; probes B, C, F–K, M, and N). Although the overall pattern of this increase was similar to that detected in 48-h T_H1-primed cells (Fig. 2*B*), we noted two striking differences. Overall, the magnitude of the AcK9/14 increase averaged 3.5-fold higher with T_H2 vs. T_H1 priming, correlating with the differentially enhanced level of the induced *Il4* and *Il13* transcriptional response (Fig. 1). Comparable AcK9/14 signals were observed for the control gene *G6pd*, demonstrating the specificity of this effect (data not shown). Second, at site *L* near the naïve/T_H1/T_H2-shared/constitutive HS_{S3}, enrichment was ≈15-fold higher in T_H2- vs. T_H1-primed cells, suggesting that this site might be a developmentally early target of priming condition-specific signals.

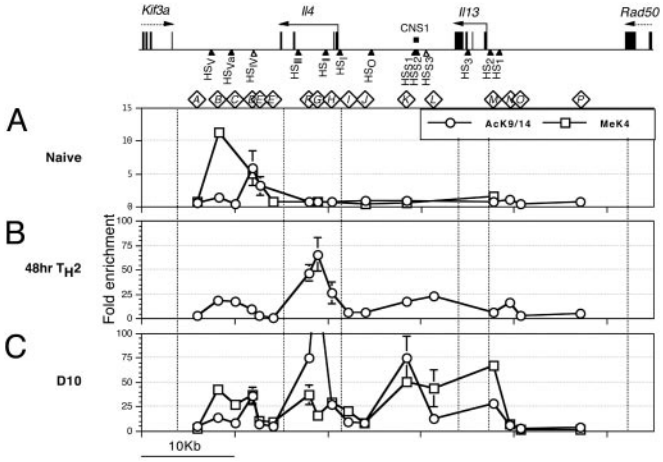

Fig. 3. Histone H3 modification at the *Il4–Il13* locus during T_H2 development. Shown are ChIP plots depicting fold-enrichment for AcK9/14 (circles) and 2MeK4 (squares) across the *Il4–Il13* locus in $CD4^+CD62L^{Hi}$ naïve T cells (*A*), 48-h T_H1-primed $CD4^+$ T cells (*B*), and resting D10.G4 cells (*C*). Error bars are SEM of $n \geq 2$ except for the following where $n = 1$: naïve (AcK9/14, sites F–H and P; 2MeK4, sites A, E′, and J). In *C*, the AcK9/14 enrichment for probe G is 150 ± 30. 2MeK4 data are not shown for 48-h-primed cells. The top of the figure is as described for Fig. 2. The naïve plot (*A*) is the same as shown in Fig. 2*A*.

Next, to ask whether the enhanced *Il4* and decreased *Il13* transcriptional potential (relative to 48-h T_H2-primed cells) observed in the T_H2 clone D10.G4 (Fig. 1*B*) correlated with changes in AcK9/14 levels, we ChIP-scanned resting D10.G4 cells for AcK9/14. Interestingly, we observed some locations in the *Il4–Il13* locus where AcK9/14 levels increased (Fig. 3 *B* and *C*; probes K and M) and others where they decreased (Fig. 3 *B* and *C*; probes B, C, and N). The most striking increases were at CNS1 (probe K, 4.3-fold) and the *Il13* promoter proximal region (probe M, 4.7-fold), whereas decreases >2-fold occurred at HS_{Va} (probe C, 2.5-fold) and the *Il13* promoter distal region (probe N, 3.3-fold). AcK9/14 levels at other locations remained fairly constant. To compare the pattern of AcK9/14 with other permissive H3 modifications, we performed ChIP analysis of resting D10.G4 cells with antibodies to 2MeK4 and PhS10. The locus-wide distributions of 2MeK4 and PhS10 were both grossly similar to the distribution of AcK9/14 (Figs. 3*C* and 5). However, there were two notable differences. First, the 2MeK4 distribution was skewed toward the outer margins of the locus, showing the greatest levels of enrichment at HS_V and the *Il13* promoter proximal region (Fig. 3*C*; probes B and M). PhS10, on the other hand, appeared to diminish on the *Rad50*-side while remaining elevated on the *Kif3a* side of the locus. These subtle differences in locus-wide distribution suggest that the different permissive H3 modifications, although overlapping perhaps in some functions, may also diverge in others. In addition, the assortment of changes in AcK9/14 levels between 48-h T_H2-primed cells and the T_H2 clone D10.G4 suggest that the regulatory elements in the *Il4–Il13* locus interact in complex ways to achieve specific degrees of *Il4* and *Il13* transcriptional permissivity.

To test whether the pattern of H3 modification detected in T_H2 cells reflects a stable change in the transcriptional state of the locus or a dynamic response to *Il4* and *Il13* transcriptional activity, we compared AcK9/14 and 2MeK4 ChIP scans of resting and 4-h-activated D10.G4 cells. For both permissive H3 modifications, the average magnitude of activation-induced increases across the *Il4–Il13* locus did not exceed 1.4-fold (Fig. 4), whereas, by comparison, *Il4* and *Il13* transcription increased >1,000-fold (Fig. 1*B* and data not shown). These results indicate that T_H2-dependent permissive

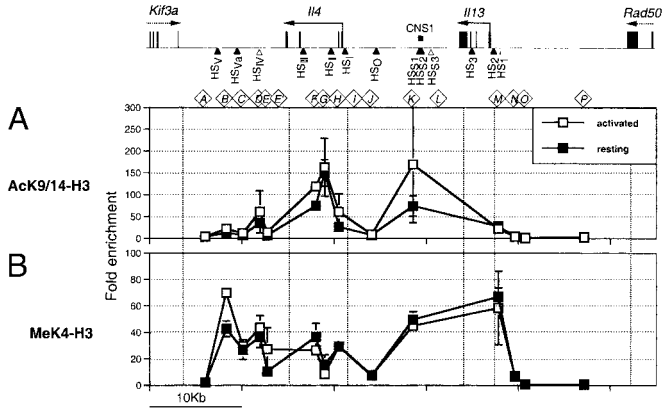

Fig. 4. Effect of activation on H3 modification at the *Il4–Il13* locus of a T_H2 clone. Shown are ChIP plots depicting fold-enrichment for AcK9/14 (*Upper*) and 2MeK4 (*Lower*) across the *Il4–Il13* locus of D10.G4 resting (filled squares) or after 4-h culture with PMA/ionomycin (open squares). Error bars are SEM of $n = 2$ for activated and $n \geq 3$ for resting. Resting data are from Fig. 3*C*. The top of the figure is as described for Fig. 2.

H3 modifications at the *Il4–Il13* locus reflect the potential for *Il4* and *Il13* transcription rather than ongoing transcriptional activity itself.

Discussion

In naïve T cells, only HS_V and HS_{IV} contained permissive H3 modifications. Our analysis revealed HS_V to be the only region of the *Il4–Il13* locus where permissive H3 modification correlated perfectly with the transcriptional states of *Il4* and *Il13*. Thus, in naïve T cells, HS_V is likely to play the key role in mediating the transcriptional permissivity of *Il4* and *Il13*. Consistent with this, HS_V is the only region of the *Il4* locus in naïve $CD4^+$ T cells to exhibit DNA hypomethylation (20). T_H2-primed $CD4^+$ T cells homozygous for a deletion encompassing HS_V ($HS_{V/Va}{}^{-/-}$) exhibit impaired *Il4* and *Il13* expression (7), suggesting that the role of HS_V in mediating *Il4* and *Il13* transcriptional permissivity may extend beyond the naïve cell stage.

How might activities recruited to HS_V act? The unusual occurrence of 2MeK4 at HS_V in naïve T cells without accompanying AcK9/14 (Fig. 2*A*; probe B) may be significant. This $2MeK4^+/AcK9/14^-$ signature has been described previously in the context of rearranging antigen-receptor gene segments and was suggested to delineate boundaries separating permissive from repressive chromatin (21). Given its status as the centromeric-most distal HS of the *Il4–Il13* locus, it is possible that HS_V participates in establishing a similar boundary between alternate chromatin states of *Kif3a* and *Il4*. Based on the unperturbed T_H2-specific pattern of DNase I hypersensitivity at the *Il4* locus of T_H2-primed $HS_{V/Va}{}^{-/-}$ $CD4^+$ T cells, it has been suggested that $HS_{V/Va}$ acts without influencing chromatin structure. However, given that only HSs proximal to HS_{II} were examined (7), it will be necessary to extend analysis of $HS_{V/Va}{}^{-/-}$ cells to more distal regions including the CNS1 element (a deletion of which also causes impaired *Il4* and *Il13* expression; ref. 6) before a chromatin structural role for HS_V can be ruled out. Although nuclear factor of activated T cells (NFAT) and GATA-3 have been detected by ChIP to bind the neighboring HS_{Va} in activated T_H2-primed cells (12, 16), it is not known what factors associate *in vivo* with HS_V in naïve T cells. The occurrence of 2MeK4 and DNA hypomethylation at HS_V precede the occurrence of DNase I hypersensitivity which only appears after T_H2-priming (4), suggesting that regulatory elements may be activated without the appearance of overt DNase I hypersensitivity. It will be informative to test whether the postulated role of HS_V in the maintenance of *Il4–Il13* locus transcriptional permissivity is established developmentally or is maintained actively through continuous transduction of tonic signals.

Based on finding similar histone acetylation at the *Il4–Il13* locus in 48-h T_H1- and T_H2-primed cells, it has been suggested that T_H-development proceeds in two successive developmental stages (12, 13). The first (before 48 h) is triggered by T cell receptor (TCR) engagement and induces permissive chromatin modifications at the *Il4–Il13* locus and transcription of *Il4* and *Il13*. The second (after 48 h) requires cytokine signaling and either stabilizes/enhances (T_H2-priming) or reverses (T_H1-priming) the changes initiated in stage 1. Our data are inconsistent with this model as we find AcK9/14 levels across the *Il4–Il13* locus (Figs. 2*B* and 3*B*) as well as *Il4* and *Il13* expression levels (Fig. 1 *A* and *B*) are significantly lower in 48-h-primed cells exposed to T_H1- as opposed to T_H2-conditions. Thus, by 48 h, cytokine signaling has already had a significant impact on both chromatin structure and gene expression. The divergent results may be due to differences in cell priming conditions or in the exact timing of cell recovery. Alternatively, the qualitative ChIP assay used in previous studies may have minimized differences in levels of chromatin modification in T_H1- and T_H2-primed cells. In support of the notion that cytokine receptor signals act from the very earliest stages of T cell differentiation, a recent study employing human IL4 receptor transgenic mice showed that effective T_H2 differentiation depends on IL4 signals being delivered during the first 48 h of priming (22). Resolution of this issue is significant, as it bears on whether TCR and cytokine receptor signaling pathways act simultaneously or successively in the specification of chromatin states.

Our analysis also shows that T_H1-priming-dependent transcriptional repression of *Il4* and *Il13* is developmentally delayed, requiring >48 h for its establishment. During this period, *Il4* and *Il13* transcriptional permissivity remain at or above the levels displayed by naïve $CD4^+$ T cells. Transcriptional repression of *Il4* and *Il13* was only detected in the T_H1 clone A.E7 (Fig. 1*A*) and correlated with the loss of permissive H3 modifications from the majority of the *Il4–Il13* locus except at HS_{IV}. To our knowledge, a developmental delay in transcriptional repression of *Il4* and *Il13* has not been described, previous studies either focusing on IL4 protein expression or not directly comparing early *Il4* mRNA expression between naïve and T_H1-primed cells.

Although *Il4* and *Il13* transcriptional repression was developmentally delayed, we still detected rapid occurrence of T_H1-priming-specific effects at the chromatin structural level. As described above, 48 h after the onset of priming, levels of AcK9/14 across the *Il4–Il13* locus were lower in cells exposed to T_H1 as opposed to T_H2 conditions, particularly at HS_{S3}, where levels were reduced >15-fold. Whether, at a time before 48 h, AcK9/14 levels were comparable and then diminished specifically with T_H1-priming or, from the outset, increased to a lesser degree with T_H1-priming is not clear from our results. Regardless of the precise trajectory of AcK9/14 levels early in the course of T_H1 priming, it is clear that the comparatively smaller increase in permissive H3 modifications in 48-h T_H1-primed cells was insufficient to support transcriptional repression. Nonetheless, the T_H1-priming-specific pattern of permissive H3 modifications observed at 48 h may be necessary for the later establishment of the transcriptionally repressed state.

HS_{IV} is exceptional in that it is the only element at the *Il4–Il13* locus where permissive H3 modifications occurred in naïve, T_H1, and T_H2 cells (Figs. 2, 3, and 5). In addition, levels of AcK9/14 at HS_{IV} increased over the course of both T_H1 and T_H2 development (Figs. 2 and 3; probe D). Preliminary results indicate that HS_{IV} is free of repressive H3 modifications in both T_H1 and T_H2 cells, but not naïve $CD4^+$ T cells (A.B., unpublished data). Thus, if we assume that the constellation of H3 modifications at a given regulatory element reflects its activation state, HS_{IV} is likely to be active in both T_H1 and T_H2 cells, but not in

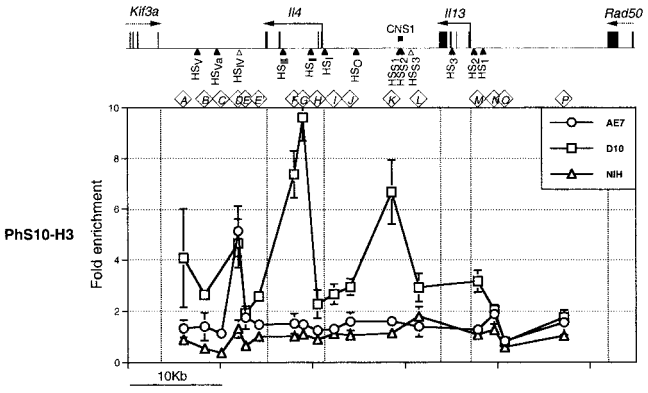

Fig. 5. Distribution of serine 10 phosphorylation on histone H3 in A.E7, D10.G4, and NIH3T3 cells. Shown are ChIP plots depicting fold-enrichment of PhS10 across the *Il4–Il13* locus of resting A.E7 (circles), D10.G4 (squares), and NIH3T3 (triangles) cells. Error bars are SEM of $n \geq 3$. The top of the figure is as described for Fig. 2.

naïve CD4$^+$ T cells. A property shared among T_H1 and T_H2 clones is irreversibility of *Il4* and *Il13* transcriptional states (23). Therefore, we speculate that HS_{IV} plays a role in maintaining transcription state stability of *Il4* and *Il13* in both T_H1 and T_H2 cells. Evaluation of this hypothesis must await targeted deletion of HS_{IV}. Interestingly, even though DNase I hypersensitivity at HS_{S3} is reported to be like HS_{IV} (constitutive and shared among naïve, T_H1 and T_H2 cells) (3), permissive H3 modifications at HS_{S3} appeared to be T_H2-specific (Figs. 2 and 3 *B* and *C*; probe L), suggesting a function that is not analogous to HS_{IV}. Alternatively, it is possible that our probe L (although only 370 bp away from HS_{S3}) may be insensitive to highly localized structures associated with HS_{S3}.

Not all regions in the *Il4–Il13* locus of T_H2-primed cells showed increases in permissive H3 modifications. The exceptions were at the outermost flanks of the locus (Figs. 3 *B* and *C* and 5; probes A, O, and P) and regions 5′ and 3′ of *Il4* (Figs. 3 *B* and *C* and 5; probes E′ and J). These hypomodified regions suggest structural compartmentalization of the locus into three domains: an *Il4* regulatory domain (encompassing HS_V through HS_{IV}), an *Il4* domain (encompassing the *Il4* transcription unit through HS_O), and an *Il13* domain (encompassing CNS1 through HS_1). A structural motif comprising a linked trio of HSs, two T_H2-specific and the other shared among naïve, T_H1 and T_H2 cells, occurs twice within the locus: once 3′ of *Il4* (HS_V/HS_{Va} and HS_{IV}) and then again 3′ of *Il13* (HS_{S1}/HS_{S2} and HS_{S3}). Given this structural parallel, we speculate that there may be an additional domain boundary between HS_{S3} and the *Il13* transcription unit that demarcates an *Il13* regulatory domain (encompassing CNS1 through HS_{S3}) from an *Il13* domain (encompassing the *Il13* transcription unit through HS_1). Finer resolution ChIP analysis will be necessary to address this possibility. Transcription of the genes flanking the *Il4–Il13* locus (*Kif3a* and *Rad50*) is similar in naïve, T_H1 and T_H2 cells (Fig. 1 *A* and *B*). Thus, from the standpoint of ensuring proper regulation of adjacent genes subject to independent transcriptional control, it makes sense that the *Il4–Il13* locus should be structurally segregated from the flanking *Kif3a* and *Rad50* genes. However, the function of subdivisions within the *Il4–Il13* locus is not immediately obvious. One possibility is that boundaries may be differentially activated at late stages of CD4$^+$ T cell differentiation when, on a given chromosome, *Il4* and *Il13* can adopt dissimilar transcriptional states (24). Resolution of these issues will be aided by the generation and chromosome-specific analysis of *Il4/Il13*-expressing T cell clones in which a single gene copy of either *Il4* or *Il13* is transcriptionally silent.

Our data are consistent with a model of *Il4* and *Il13* transcriptional state specification that is driven by an ordered sequence of regulatory element activation/de-activation events. At the naïve stage, preactivation of HS_V suffices to maintain low levels of *Il4* and *Il13* transcriptional permissivity. Synergistic activation of the 3′ *Il4* and CNS1 enhancers during T_H2-priming leads to high level *Il4* and *Il13* transcriptional permissivity. Temporally delayed deactivation of both the 3′ *Il4* and CNS1 enhancers with T_H1-priming leads to *Il4* and *Il13* transcriptional repression. Temporally delayed activation of HS_{IV} "locks in" the transcriptional states of silence and permissivity in T_H1 and T_H2 cells, respectively. Definitive assessment of this model will require studies of the direct *cis* effects of specific regulatory element deletions on chromatin structure and transcription as well as identification of factors that mediate the functional effects of each regulatory element.

We thank Yan Zhang, Jennifer Epler, Thomas Arroll, and Heather Shilling for excellent technical assistance; Mark Groudine and his laboratory for teaching us how to perform ChIP assays; Anton Krumm for thoughtful discussions; and Chris Wilson, Amy Weinmann, Joonsoo Kang, and Heather Shilling for critical reading of the manuscript. M.B. thanks L. J. Bix-Daw and D. E. Daw for their support. This study was supported by grants to M.B. from the National Institutes of Health, the Burroughs Wellcome Foundation, the Cancer Research Institute, the Cystic Fibrosis Foundation, and the Marion Smith Endowment.

1. Reiner, S. & Locksley, R. (1995) *The Regulation of Immunity to Leishmania Major* (Annual Reviews, Palo Alto).
2. Urban, J. F., Jr., Madden, K. B., Svetic, A., Cheever, A., Trotta, P. P., Gause, W. C., Katona, I. M. & Finkelman, F. D. (1992) *Immunol. Rev.* **127,** 205–220.
3. Takemoto, N., Koyano-Nakagawa, N., Yokota, T., Arai, N., Miyatake, S. & Arai, K. (1998) *Int. Immunol.* **10,** 1981–1985.
4. Agarwal, S. & Rao, A. (1998) *Immunity* **9,** 765–775.
5. Lee, G. R., Fields, P. E., Griffin, T. J. & Flavell, R. A. (2003) *Immunity* **19,** 145–153.
6. Mohrs, M., Blankespoor, C. M., Wang, Z. E., Loots, G. G., Afzal, V., Hadeiba, H., Shinkai, K., Rubin, E. M. & Locksley, R. M. (2001) *Nat. Immunol.* **2,** 842–847.
7. Solymar, D. C., Agarwal, S., Bassing, C. H., Alt, F. W. & Rao, A. (2002) *Immunity* **17,** 41–50.
8. Strahl, B. D. & Allis, C. D. (2000) *Nature* **403,** 41–45.
9. Fischle, W., Wang, Y. & Allis, C. D. (2003) *Curr. Opin. Cell Biol.* **15,** 172–183.
10. Khorasanizadeh, S. (2004) *Cell* **116,** 259–272.
11. Makar, K. W., Perez-Melgosa, M., Shnyreva, M., Weaver, W. M., Fitzpatrick, D. R. & Wilson, C. B. (2003) *Nat. Immunol.* **4,** 1183–1190.
12. Avni, O., Lee, D., Macian, F., Szabo, S. J., Glimcher, L. H. & Rao, A. (2002) *Nat. Immunol.* **3,** 643–651.
13. Fields, P. E., Kim, S. T. & Flavell, R. A. (2002) *J. Immunol.* **169,** 647–650.
14. Kaye, J., Porcelli, S., Tite, J., Jones, B. & Janeway, C. A., Jr. (1983) *J. Exp. Med.* **158,** 836–856.
15. Hecht, T. T., Longo, D. L. & Matis, L. A. (1983) *J. Immunol.* **131,** 1049–1055.
16. Agarwal, S., Avni, O. & Rao, A. (2000) *Immunity* **12,** 643–652.
17. Loots, G. G., Locksley, R. M., Blankespoor, C. M., Wang, Z. E., Miller, W., Rubin, E. M. & Frazer, K. A. (2000) *Science* **288,** 136–140.
18. Hural, J. A., Kwan, M., Henkel, G., Hock, M. B. & Brown, M. A. (2000) *J. Immunol.* **165,** 3239–3249.
19. Grogan, J. L., Wang, Z. E., Stanley, S., Harmon, B., Loots, G. G., Rubin, E. M. & Locksley, R. M. (2003) *J. Immunol.* **171,** 6672–6679.
20. Lee, D. U., Agarwal, S. & Rao, A. (2002) *Immunity* **16,** 649–660.
21. Morshead, K. B., Ciccone, D. N., Taverna, S. D., Allis, C. D. & Oettinger, M. A. (2003) *Proc. Natl. Acad. Sci. USA* **100,** 11577–11582.
22. Seki, N., Miyazaki, M., Suzuki, W., Hayashi, K., Arima, K., Myburgh, E., Izuhara, K., Brombacher, F. & Kubo, M. (2004) *J. Immunol.* **172,** 6158–6166.
23. Grogan, J. L., Mohrs, M., Harmon, B., Lacy, D. A., Sedat, J. W. & Locksley, R. M. (2001) *Immunity* **14,** 205–215.
24. Kelly, B. L. & Locksley, R. M. (2000) *J. Immunol.* **165,** 2982–2986.